International Journal of Modern Physics C
Vol. 16, No. 12 (2005) 1819–1830


World Scientific
www.worldscientific.com

# THREE-DIMENSIONAL LATTICE BOLTZMANN MODEL RESULTS FOR COMPLEX FLUIDS ORDERING

G. AMATI* and F. MASSAIOLI†

*CASPUR, Via dei Tizii 6/b, 00185 Rome, Italy*
**g.amati@caspur.it*
†*f.massaioli@caspur.it*

G. GONNELLA‡ and AIGUO XU§

*Dipartimento di Fisica, Università di Bari, and INFN, Sezione di Bari*
*Via Amendola 173, 70126 Bari, Italy*
‡*gonnella@ba.infn.it*
§*aiguoxu@yuragi.jinkan.kyoto-u.ac.jp*

A. LAMURA

*Istituto Applicazioni Calcolo, CNR, Sezione di Bari*
*Via Amendola 122/D, 70126 Bari, Italy*
*a.lamura@ba.iac.cnr.it*

Received 5 May 2005
Revised 8 June 2005

The kinetics of domain growth of fluid mixtures quenched from a disordered to a lamellar phase has been studied in three dimensions. We use a numerical approach based on the lattice Boltzmann method (LBM). A novel implementation for LBM which "fuses" the collision and streaming steps is used in order to reduce memory and bandwidth requirements. We find that extended defects between stacks of lamellae with different orientation dominate the late time dynamics.

*Keywords*: Lattice Boltzmann method; parallel code; lamellar phase; complex fluids.

PACS Nos.: 47.11.+j, 64.75.+g, 47.54.+r, 05.70.Ln.

## 1. Introduction

Hydrodynamics is an essential ingredient in the modelling of complex fluids. Many relevant phenomena in soft matter physics depend on the interplay between the mesoscopic structures in the fluid (interfaces, extended objects like polymers, colloidal particles, etc.) and the local velocity field.[1]

§Present address: Division of Physics and Astronomy, Yoshida-south Campus, Kyoto University, Kyoto 606-8501, Japan.

For example, it is well known that the presence of the velocity field affects the process of phase separation of fluid mixtures quenched below the critical point. Different power-law regimes for the growth of the average size $R(t)$ of the domains of the separating phases are found for different ranges of viscosity. At high viscosity, when diffusion is the physical mechanism operating in phase segregation, one has $R \sim t^{1/3}$. At lower viscosities, the coupling between surface tension and the velocity field becomes relevant and, depending on if inertial or viscous terms dominate in the Navier–Stokes equation, one has $R \sim t^{2/3}$ or $R \sim t$, respectively.[2] Other examples come from the study of rheological properties.[1] For instance, in shear banding, two phases, one of them metastable or not existing in equilibrium, coexist in a Couette cell having different velocity profiles.[3] This phenomenon can be described only if the dynamics of the velocity field is taken into account.

The most appropriate approach for describing a given complex fluid system depends on the time and the length scales under investigations. In the study of the dynamics of mesoscopic structures and phase transitions, a microscopic approach would become prohibitive from the computational point of view and coarse-grained models are often more convenient. In this paper we study the ordering properties of a fluid with lamellar configurations whose dynamics is described by a time dependent convection-diffusion equation coupled to the Navier–Stokes equation. The equilibrium properties of the lamellar phase are described by a free-energy model particularly appropriate for di-block copolymers in the weak segregation limit.[4]

We use lattice Boltzmann method (LBM)[5] to solve both the dynamical equations presenting a new implementation for LBM which "fuses" the collision and streaming steps to reduce memory and bandwidth requirements. This is not the only possibility when dealing with the numerical solution of a convection-diffusion equation coupled with the Navier–Stokes equation. Indeed, several approaches have been proposed. Finite difference (FD) schemes have been adopted, in the case of thermal lattice Boltzmann models for a single fluid[6] and for multiphase flows, to solve the temperature equation.[7] FD schemes have been used also to solve the dynamics of passive scalars by LBM for fluid flows.[8] An updated discussion on this specific issue can be found in Ref. 9. While, in general, FD schemes can reduce the amount of required memory, in LBM boundary conditions are more easily implemented and give better numerical stability. Moreover, LBM has a more detailed microscopic description than a FD scheme because the LBM takes into consideration the velocities of the particles.[10] This aspect could be useful when dealing with mixtures of two fluids with different viscosity and/or mass.

Unlike the case of simple binary mixtures, the problem of lamellar ordering is not well understood and there are no quantitative results for the three-dimensional case. Lamellar order is typical of systems with competing interactions.[11,12] Examples are di-block copolymer melts, where chains of type A and B, covalently bonded end-to-end in pairs, segregate at low temperatures in regions separated by a stack of lamellae,[13] ternary mixtures where surfactant form interfaces between oil and water,[14] or smectic liquid crystals.[15]

The ordering of lamellar systems is affected by the presence of defects on large scales. Previous studies showed the relevance of hydrodynamics on this process for two-dimensional systems.[11,12,16,17] In particular it was found that characteristic lengths evolve with a complex time dependence. A pre-asymptotic regime with a growth consistent with a power-law behavior is followed later by slower logarithmic growth.[17] This behavior can be interpreted as due to the dynamics of grain boundary defects between domains of differently oriented lamellae. We show in this paper that extended defects also have a prominent role in the three-dimensional case.

The paper is organized as follows. Next section decribes the model and the Lattice Boltzmann equation we used. In Sec. 3, the implementation of the algorithm is briefly presented. Results for lamellar ordering are described in Sec. 4.

## 2. The Model

The time evolution of our system is described by two phenomenological equations.[18] The convection-diffusion equation for the order parameter $\varphi$, which represents the concentration difference between the two components of the mixture, is

$$\partial_t \varphi + \boldsymbol{\nabla} \cdot (\varphi \mathbf{v}) = \Gamma\Theta \nabla^2 \mu \,, \tag{1}$$

where $\mu$ is the chemical potential difference between the two components, $\Gamma\Theta$ is a mobility coefficient and $\mathbf{v}$ is the local fluid velocity. It obeys the Navier–Stokes equation which, in the incompressibility limit $\boldsymbol{\nabla} \cdot \mathbf{v} = 0$, reads as

$$\partial_t v_\alpha + \mathbf{v} \cdot \boldsymbol{\nabla} v_\alpha = -\frac{1}{n} \partial_\beta P^{th}_{\alpha\beta} + \nu \nabla^2 v_\alpha \tag{2}$$

where $n$ is the total density, $\nu$ is the kinematic viscosity, and $P^{th}_{\alpha\beta}$ is the thermodynamic pressure tensor. The pressure tensor and the chemical potential difference can be calculated from an appropriate free-energy functional by using the formulae $P^{th}_{\alpha\beta} = \{n\delta F/\delta n + \varphi \delta F/\delta\varphi - f(n,\varphi)\}\delta_{\alpha\beta} + D_{\alpha\beta}$ and $\mu = \delta F/\delta\varphi$, where $f(n,\varphi)$ is the free-energy density and a symmetric tensor $D_{\alpha\beta}$ has to be added to ensure that the condition of mechanical equilibrium $\partial_\alpha P^{th}_{\alpha\beta} = 0$ is satisfied.[19] Their full expressions can be found in Ref. 12.

We use a lattice Boltzmann scheme based on the $D3Q15$ lattice,[20] where $D3$ denotes the number of spatial dimensions and $Q15$ the number of lattice speeds, to solve the Navier–Stokes equation. A set of two distribution functions $f_i(\mathbf{r},t)$ and $g_i(\mathbf{r},t)$ is defined on each lattice site $\mathbf{r}$ at each time $t$. Each of them is associated with a velocity vector $\mathbf{e}_i$. We will denote by the index $I$, the 6 velocity vectors $\mathbf{e}_i$ having modulus $|\mathbf{e}_i^I| = \Delta x/\Delta t = c$ and by the index $II$, the 8 velocity vectors $\mathbf{e}_i$ having modulus $|\mathbf{e}_i^{II}| = \sqrt{3}c$, with $\Delta x$ being the lattice step and $\Delta t$ the time step. The function $f_0(\mathbf{r},t)$, corresponding to the distribution component that does not propagate ($\mathbf{e}_0 = \mathbf{0}$), is also taken into account. They evolve according to a single relaxation-time Boltzmann equation[21]:

$$f_i(\mathbf{r} + \mathbf{e}_i \Delta t, t + \Delta t) - f_i(\mathbf{r},t) = -\frac{1}{\tau_f}[f_i(\mathbf{r},t) - f_i^{\mathrm{eq}}(\mathbf{r},t)] \,, \qquad i = 0,1,\ldots,14 \tag{3}$$

where $\tau_f$ is a relaxation parameter and $f_i^{\rm eq}(\mathbf{r},t)$ are local equilibrium distribution functions. A similar equation holds for $g_i(\mathbf{r},t)$. The distribution functions $f_i$ are related to the total density $n$ and to the fluid momentum $n\mathbf{v}$ through $n=\sum_{i=0}^{14} f_i$ and $n\mathbf{v}=\sum_{i=0}^{14} f_i\mathbf{e}_i$. These quantities are locally conserved in any collision process and, therefore, we require that the local equilibrium distribution functions fulfil the equations $\sum_{i=0}^{14} f_i^{\rm eq}=n$ and $\sum_{i=0}^{14} f_i^{\rm eq}\mathbf{e}_i=n\mathbf{v}$, and the further constraint $\sum_{i=0}^{14} f_i^{\rm eq}e_\alpha e_\beta = c^2P_{\alpha\beta}+nv_\alpha v_\beta$. The distribution functions $g_i$ are related to the order parameter $\varphi$ and the fluid velocity through $\varphi=\sum_{i=0}^{14} g_i$ and $\varphi\mathbf{v}=\sum_{i=0}^{14} g_i\mathbf{e}_i$. The order parameter $\varphi$ is locally conserved in any collision process and, therefore, we require that the local equilibrium distribution functions fulfil the equation $\sum_{i=0}^{14} g_i^{\rm eq}=\varphi$ and the further constraints $\sum_{i=0}^{14} g_i^{\rm eq}\mathbf{e}_i=\varphi\mathbf{v}$ and $\sum_{i=0}^{14} g_i^{\rm eq}e_\alpha e_\beta = c^2\Gamma\mu\delta_{\alpha\beta}+\varphi v_\alpha v_\beta$.[22,23]

The local equilibrium distribution functions can be expressed as an expansion at the second order in the velocity $\mathbf{v}$[20]:

$$\begin{aligned}
f_0^{\rm eq} &= A_0 + C_0 v^2\,,\\
f_i^{\rm eq} &= A_I + B_I v_\alpha e_{i\alpha} + C_I v^2 + D_I v_\alpha v_\beta e_{i\alpha}e_{i\beta} + G_{I,\alpha\beta}e_{i\alpha}e_{i\beta}\,, \quad i=1,\ldots,6\,,\\
f_i^{\rm eq} &= A_{II} + B_{II} v_\alpha e_{i\alpha} + C_{II} v^2 + D_{II} v_\alpha v_\beta e_{i\alpha}e_{i\beta} + G_{II,\alpha\beta}e_{i\alpha}e_{i\beta}\,, \quad i=7,\ldots,14
\end{aligned} \tag{4}$$

and similarly for the $g_i^{\rm eq}$, $i=0,\ldots,14$. The constraints on the equilibrium distribution functions can be used to fix the coefficients of these expansions. A suitable choice of the coefficients in the expansions (4) is

$$A_0 = n - 56A_{II}\,, \qquad A_I = 8A_{II}\,, \qquad A_{II} = \frac{P_{\alpha\beta}\delta_{\alpha\beta}}{72}\,, \tag{5}$$

$$B_I = 8B_{II}\,, \qquad B_{II} = \frac{n}{24c^2}\,, \tag{6}$$

$$C_0 = -\frac{n}{3c^2}\,, \qquad C_I = 8C_{II}\,, \qquad C_{II} = -\frac{n}{48c^2}\,, \tag{7}$$

$$D_I = 8D_{II}\,, \qquad D_{II} = \frac{n}{16c^4}\,, \tag{8}$$

$$G_{I,\alpha\beta} = 8G_{II,\alpha\beta}\,, \qquad G_{II,\alpha\beta} = \frac{P_{\alpha\beta}-\frac{1}{3}P_{\sigma\sigma}\delta_{\alpha\beta}}{16c^2}\,. \tag{9}$$

The expansion coefficients for the $g_i^{\rm eq}$ can be obtained from the previous ones with the formal substitutions $n\to\varphi$ and $P_{\alpha\beta}\to\Gamma\mu\delta_{\alpha\beta}$. By using a multi-scale expansion, it can be shown that the above described lattice Boltzmann scheme simulates at second order the continuity in $\Delta t$, the quasi-incompressible Navier–Stokes with the kinematic viscosity $\nu$ given by $\nu=(c^2/3)\Delta t(\tau_f-1/2)$, and the convection-diffusion equation with $\Theta=c^2\Delta t(\tau_g-1/2)$.

The free energy considered in this work is

$$F=\int d\mathbf{r}\left[\frac{1}{3}n\ln n+\frac{a}{2}\varphi^2+\frac{b}{4}\varphi^4+\frac{\kappa}{2}(\nabla\varphi)^2+\frac{d}{2}(\nabla^2\varphi)^2\right]. \tag{10}$$

The term in $n$ gives rise to a positive background pressure and does not affect the phase behavior. The terms in $\varphi$ correspond to the Brazovskii free energy.[24] We take $b$, $d > 0$ to ensure stability. For $a > 0$ the fluid is disordered; for $a < 0$ it adopts an ordered state whose nature depends on the value of $\kappa$. Indeed, for positive values of $\kappa$ the two homogeneous phases with $\varphi = \pm\sqrt{-a/b}$ coexist, while for $\kappa < 0$ there is a transition, when $b = -a$, where $a \approx -1.11\kappa^2/d$, into a lamellar state with characteristic wave-vector $q = \sqrt{-\kappa/2d}$.[17]

## 3. The "Fused" LBM Implementation

Large scale 3D simulations, usually needed in phase ordering studies, demand significant computational requirements. Customary LBM implementations are subjected to a trade-off between the memory occupation and the amount of memory accesses needed.

The use of two complete lattice representation allow for an evolution step to be performed in a single pass, reading populations from one lattice, computing the post collisional values, and writing them in the proper places in the other lattice copy. Computational efficiency comes at the price of doubling the amount of memory needed for the simulation.

A compact storage implementation, using a single lattice copy, is possible, but data dependencies arise, which have to be removed by splitting the LBM evolution into two steps: local collisions are computed first, storing the post collisional values in the same lattice site, then streaming is performed by explicit memory-to-memory copies. This approach doubles the number of memory load and stores, thus lowering the overall computational efficiency. Moreover, parallel scalability on shared memory multiprocessor systems is significantly hampered, as the memory subsystem has double the amount of work to perform.

For the simulation described in this paper, a D3Q15, up to $512^3$, lattice was used. Both approaches impose serious limits, on the maximum system size and on the feasible time scales respectively. We thus resorted to a newer approach,[25,26] in which an LBM evolution step is performed in a single pass and only one lattice copy is present in memory. This is made possible by using a Lagrangian approach, in which populations are held in fixed memory locations, and movements are represented by cyclical changes, at each time step, between the corresponding physical coordinates and memory location indexes (see Ref. 27 for a detailed description).

This "fused" approach increases serial performances by 20% with respect to the compact storage approach, while preserving its main benefit (a $512^3$ simulation requiring approximately 35 GB). The parallel speedup on a IBM Power 4 system at 24 on 32 CPUs (the compact storage implementation speedup being 17 on 32 CPUs).

## 4. Numerical Results

The numerical results presented here were obtained from $N = 512$ lattice sites per spatial direction and periodic boundary conditions. The following parameters

were used: $a = -b = -0.026$, $\kappa = -0.005$, $d = 0.0025$, $\Gamma = 0.25$, $\tau_f = 0.8$, $\tau_g = 1$, $\Delta x = 1$, and $\Delta t = 1$. The choice $|a| = b$ is such that the minimum of the polynomial terms in the free energy (10) is in $\varphi = \pm 1$. For the selected parameters, the lamellar is the equilibrium state. The characteristic wave-length, corresponding to the width of two adjacent lamellae of different composition, is $\lambda = 2\pi/q = 2\pi$ in units of lattice spacings. The kinematic viscosity is $\nu = 0.1$ and corresponds to a value for which hydrodynamic transport is relevant as pointed out in previous study of lamellar ordering in two dimensions.[17] The system was initialized in a disordered state with $\varphi = \varepsilon$ where $\varepsilon$ is a random number uniformly distributed in the range $[-0.1, 0.1]$.

After the sudden initial quench, the free energy drives the system into its local equilibrium configuration. At high viscosities the system remains frozen in configurations similar to that at time $t = 100\,000$ of Fig. 1. At sufficiently low viscosities, like the one considered here, the velocity field becomes effective and induces the merging of lamellae. Local defects, like channels connecting lamellae of some phase, or one-dimensional defects like disclinations or seams, are progressively eliminated. Order is then reached on larger scales as it can be seen at time $t = 600\,000$ in Fig. 1. However, extended two-dimensional defects are difficult to eliminate and are observed at the latest stages of the simulations. These defects correspond to parallel stacks of lamellae *perpendicularly* oriented with respect to each other. One-dimensional versions of these *grain boundaries* were also observed to dominate the late time evolution in previous studies of 2D lamellar ordering.[17] This is visible in Fig. 2, where a typical pattern is presented for the two-dimensional case for a long time.

A quantitative description of the ordering process comes from the analysis of the structure factor $C(\mathbf{k}, t) = \langle \varphi(\mathbf{k}, t)\varphi(-\mathbf{k}, t)\rangle$, where $\varphi(\mathbf{k}, t)$ is the Fourier transform of the order parameter $\varphi$. After the spherical average, we plotted $C(k, t)$ at different times. In the early regime, with $t \simeq 30\,000$, $C(k, t)$ develops a maximum at a momentum $k_M$ which decreases with time until the equilibrium value $q$ is reached at $t \simeq 200\,000$. Then the peak $C_M(t) = C(q, t)$, remaining at $q$, grows while the width decreases indicating an increase of order in the system. A characteristic length $L$

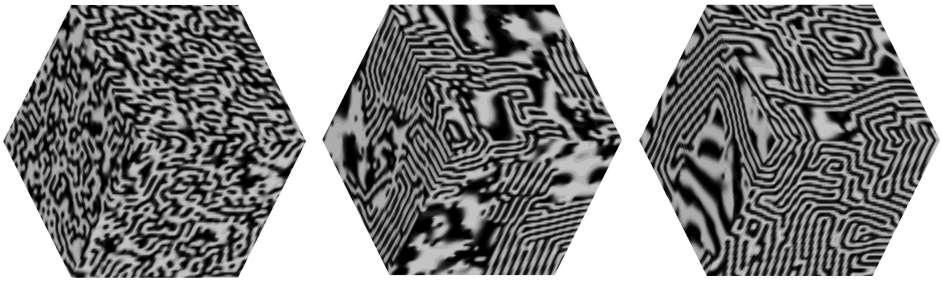

$t = 100\,000$ $t = 600\,000$ $t = 1\,000\,000$

Fig. 1. Configurations of the order parameter $\varphi$ at different times on a portion $128^3$ of the whole $512^3$ lattice.

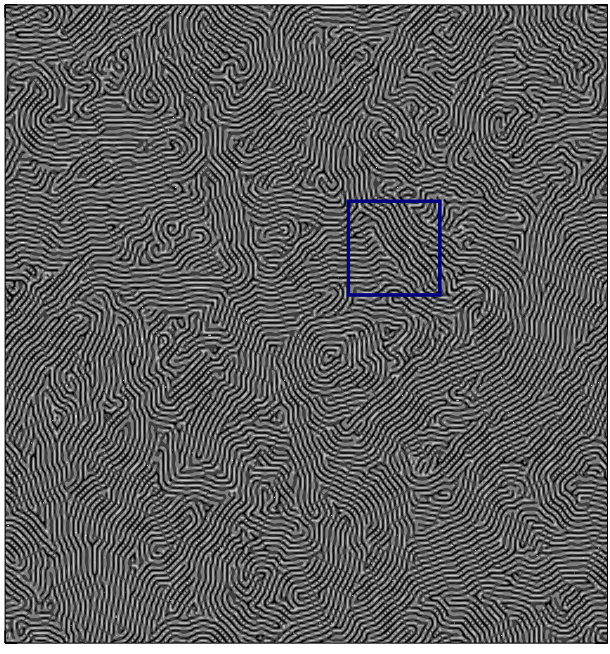

Fig. 2. Configuration of the order parameter $\varphi$ in the two dimensional case at long times on a $1024^2$ lattice. The black square highlights the presence of grain boundaries. The following parameters were used: $a = -b = -0.0002$, $\kappa = -0.0006$, $d = 0.00076$, $\Gamma\Theta = 25$, $\tau_f = 0.505$, $\Delta x = 1$, and $\Delta t = 0.2$.

for this process can be extracted from the structure factor in the usual way by measuring the full width $\delta k$ of $C(k,t)$ at half maximum and defining $L(t) = 2\pi/\delta k$. The results for the time behavior of $C_M(t)$ and $L(t)$ in the case of the $512^3$ lattice are displayed in Fig. 3. What we found is that after the initial formation of lamellae, the system increases its order as the growth of $C_M$ and $L$ in the time range [200 000, 600 000] supports. However, this interval is too short to obtain a quantitative behavior for $C_M$ and $L$. After $t \sim 600\,000$, in relation to a sudden decrease observed in $L$ and $C_M$, the further evolution of the system proceeds through distortion of the grain boundaries existing at that time. Different domains, trying to increase their size, push themselves reciprocally, helped by the velocity field. This can be seen in Fig. 4 where the velocity map at time $t = 925\,000$ is presented for a $60 \times 60$ section of the system on the $y - x$ plane. It is evident that defects tend to move towards each other, helped by the hydrodynamic flow. For example, it appears that the horizontal lamella in the bottom right part of the figure is driven towards the vertical lamellae in the left which are moving downwards. This gives an unexpected delayed increase of curvature, also observed in $D = 2$, as it can be seen in the configuration at $t = 1\,000\,000$ in Fig. 1 where lamellae are almost completely entangled. On lattices of size $N \leq 64$, complete order was almost reached.

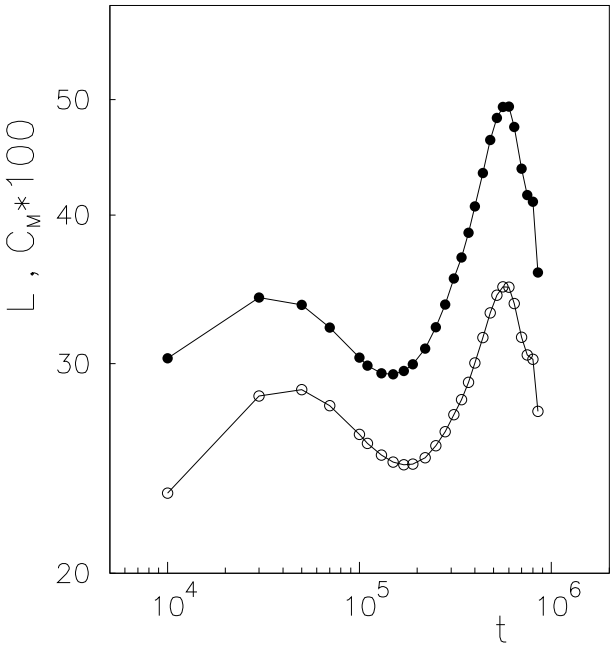


Fig. 3. Time behavior of characteristic size $L$ (•) and peak height $C_M$ (◦).

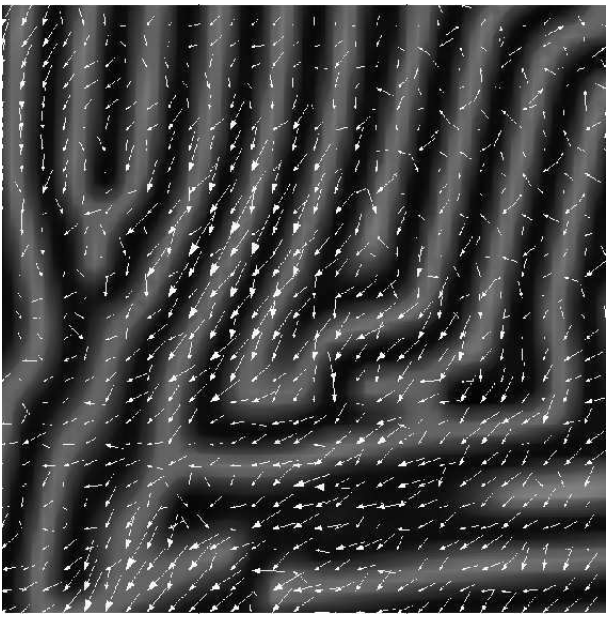

Fig. 4. Velocity field on the $y - z$ plane of a $60 \times 60$ section of the system at time $t = 925\,000$. Domains of different composition are in different tones of black and arrows are the projection of the velocity vectors $\mathbf{v}$ on the image plane.

The role of hydrodynamics is important in this process: the system can reach a higher degree of order only by developing a strong velocity field which bends the existing flat grain boundaries. This picture is confirmed by the increase of the kinetic energy per site, $E_{\rm kin}(t) = 1/2N^3 \sum_{\mathbf{r}} n(\mathbf{r},t)v^2(\mathbf{r},t)$, which is observed at $t \sim 600\,000$ in Fig. 5. After the formation of the lamellae, $E_{\rm kin}$ decreases from $t \sim 100\,000$ to $t \sim 600\,000$ and this corresponds to the time interval where the order increases in the system (see Fig. 3). From the picture, it is evident that $E_{\rm kin}$ continues to increase up to the longest simulated time $t = 1\,000\,000$. The computational cost to further continue such a run is too demanding, so we considered a run with the same set of parameters on a smaller lattice ($N = 128$) that we could follow up to $t = 10\,000\,000$. The plot of the kinetic energy density is in the inset of Fig. 5. It is remarkable that the time behavior until $t \sim 1\,000\,000$ is qualitatively and quantitatively similar to the one in the case with $N = 512$. This seems to indicate that ordering in three dimensions at long times is not so greatly affected by the size of the system, at least up to $N = 512$ since the evolution of $E_{\rm kin}$ is similar. This could be due to defects that are not removed. Indeed, as we have already said, the system orders only on lattices with $N \leq 64$. At larger time, $E_{\rm kin}$ oscillates around a constant value suggesting that the system is not able to find a more ordered configuration which dumps velocities, but stays oscillating between

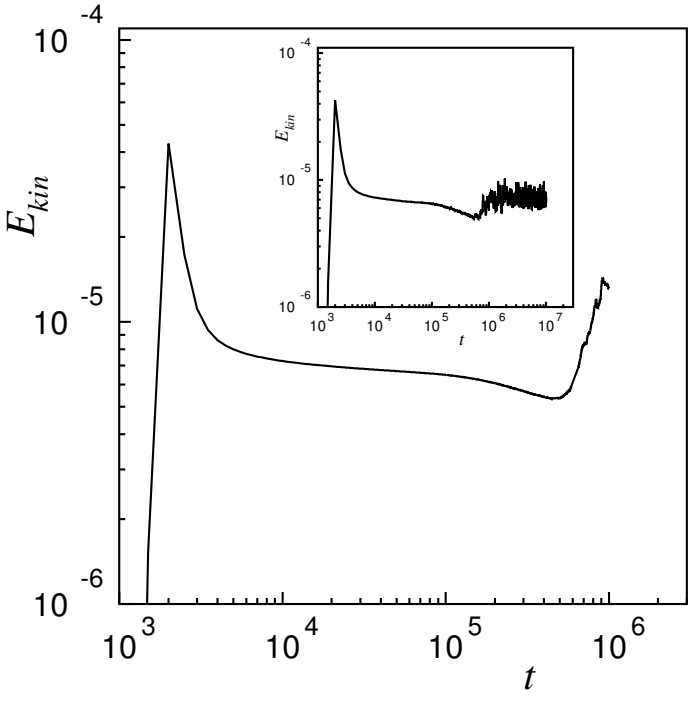


Fig. 5. Time behavior of the kinetic energy $E_{\rm kin}$ for the $512^3$ lattice. In the inset $E_{\rm kin}$ is plotted in the case of the $128^3$ lattice.

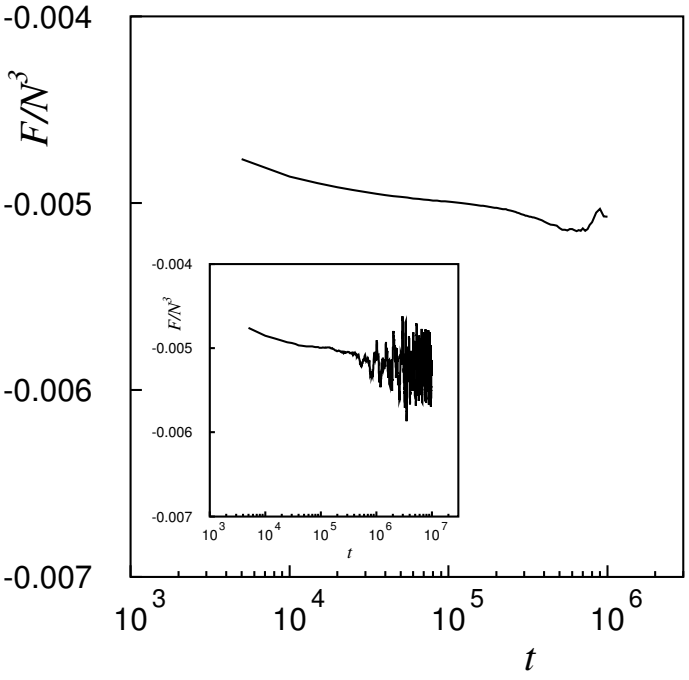


Fig. 6. Time behavior of the free energy per site $F/N^3$ for the $512^3$ lattice. In the inset, $F/N^3$ is plotted in the case of the $128^3$ lattice.

metastable states trying to eventually increase its order. We are not able to access numerically such long time limit. For the sake of completeness, we report also the time behavior of the free energy (10) per site which is plotted in Fig. 6. It appears that $F/N^3$ for both the lattice sizes ($N = 128$ and $N = 512$) has the same trend as the kinetic energy. It diminishes in same time interval where $E_{\rm kin}$ decreases since the system is approaching a more stable configuration, at $t \sim 600\,000$ it increases and then continues oscillating. In the quenching of dissipative systems, as in our case, the sum of the kinetic energy and of the free energy is expected to diminish as the equilibrium is approached. Indeed, this is what we see until $t \sim 600\,000$, then the interplay between defects and hydrodynamics produces the observed oscillating behavior.

## 5. Conclusions

We have implemented a 3D version of the lattice Boltzmann method where the collision and streaming steps are fused in a new implementation of the algorithm with the benefits of saving memory and bandwidth requirements. We have applied this LBM to study lamellar ordering. Our results show that at low viscosity, order is reached on large scales but extended defects are found to dominate the late time dynamics. Indeed, no complete order can be observed even at very long times on

large systems as a consequence of the difficulty of removing defects in three spatial dimensions.

## Acknowledgments

This work has been partially supported by MIUR (PRIN-2004).

## References

1. R. G. Larson, *The Structure and Rheology of Complex Fluids* (Oxford University Press, New York, 1999).
2. J. M. Yeomans, *Annual Review of Computational Physics VII*, ed. D. Stauffer (World Scientific, Singapore, 2000), p. 61.
3. P. D. Olmsted and C.-Y. D. Lu, *Phys. Rev. E* **56**, 55 (1997); *ibid.* **60**, 4397 (1999).
4. L. Leibler, *Macromolecules* **13**, 1602 (1980); T. Ohta and K. Kawasaki, *ibid.* **19**, 2621 (1986); G. H. Fredrickson and E. Helfand, *J. Chem. Phys.* **87**, 697 (1987).
5. F. Higuera, S. Succi and R. Benzi, *Europhys. Lett.* **9**, 345 (1989); R. Benzi, S. Succi and M. Vergassola, *Phys. Rep.* **222**, 145 (1992); S. Chen and G. D. Doolen, *Annu. Rev. Fluid Mech.* **30**, 329 (1998); S. Succi, *The Lattice Boltzmann Equation* (Oxford University Press, New York, 2001).
6. O. Filippova and D. Hänel, *Int. J. Mod. Phys. C* **9**, 1439 (1998); *J. Comput. Phys.* **158**, 139 (2000); P. Lallemand and L. S. Luo, *Phys. Rev. E* **68**, 036706 (2003).
7. R. Zhang and H. Chen, *Phys. Rev. E* **67**, 066711 (2003).
8. S. Succi, H. Chen, C. Teixeira, G. Bella, A. Mario and K. Molvig, *J. Comput. Phys.* **152**, 493 (1999).
9. I. Rasin, S. Succi and W. Miller, *J. Comput. Phys.* **206**, 453 (2005).
10. P. Albuquerque, D. Alemani, B. Chopard and P. Leone, *Lect. Notes Comput. Sc.* **3039**, 540 (2004).
11. G. Gonnella, E. Orlandini and J. M. Yeomans, *Phys. Rev. Lett.* **78**, 1695 (1997).
12. G. Gonnella, E. Orlandini and J. M. Yeomans, *Phys. Rev. E* **58**, 480 (1998).
13. F. S. Bates and G. Fredrickson, *Ann. Rev. Phys. Chem.* **41**, 525 (1990).
14. G. Gompper and M. Schick, *Phase Transitions and Critical Phenomena*, Vol. 16 (Academic Press, New York, 1994).
15. P. de Gennes, *The Physics of Liquid Crystals* (Clarendon Press, Oxford, 1974).
16. Y. Yokojima and Y. Shiwa, *Phys. Rev. E* **65**, 056308 (2002).
17. A. Xu, G. Gonnella, A. Lamura, G. Amati and F. Massaioli, *Europhys. Lett.*, cond-mat/0404205 (2004), (submitted).
18. S. R. De Groot and P. Mazur, *Non-equilibrium Thermodynamics* (Dover Publications, New York, 1984).
19. R. Evans, *Adv. Phys.* **28**, 143 (1979).
20. Y. H. Qian, D. d'Humieres and P. Lallemand, *Europhys. Lett.* **17**, 419 (1992).
21. P. Bhatnagar, E. P. Gross and M. K. Krook, *Phys. Rev.* **94**, 511 (1954).
22. M. R. Swift, E. Orlandini, W. R. Osborn and J. M. Yeomans, *Phys. Rev. E* **54**, 5041 (1996).
23. A. Xu, G. Gonnella and A. Lamura, *Phys. Rev. E* **67**, 056105 (2003).
24. S. A. Brazovskii, *Sov. Phys. JETP* **41**, 85 (1975).
25. G. Amati and F. Massaioli, *Performance portability of a Lattice Boltzmann Code*, Proceeding of IBM Scicomp9, Bologna, Italy (2004), http://www.spscicomp.org/ScicomP9/Presentations/MassaioliAmatiScicomp09.pdf.

26. G. Amati and F. Massaioli, Parallel and serial issues for a lattice Boltzmann method code: a performance point of view, *Parellel Computational Fluid Dynamics*: *Multidisciplinary Applications*, ed. G. Winter *et al.* (Elsevier Publishing Co., 2005).
27. G. Amati and F. Massaioli, *in preparation*.